



Trans. Nonferrous Met. Soc. China 32(2022) 2965-2978

Transactions of Nonferrous Metals Society of China

www.tnmsc.cn



# Interfacial pressure distribution and bonding characteristics in twin-roll casting of Cu/Al clad strip

Jun-peng ZHANG<sup>1,2</sup>, Hua-gui HUANG<sup>1,2</sup>, Jing-na SUN<sup>1,2</sup>, Ri-dong ZHAO<sup>1,2</sup>, Miao FENG<sup>1,2</sup>

- 1. National Engineering Research Center for Equipment and Technology of Cold Strip Rolling, Yanshan University, Qinhuangdao 066004, China;
  - 2. School of Mechanical Engineering, Yanshan University, Qinhuangdao 066004, China

Received 9 August 2021; accepted 20 January 2022

Abstract: The mechanical properties and product thickness specifications of bimetallic clad strip prepared by twin-roll casting are tightly related to the mechanical behavior of bonding interface interaction. The thermal—flow coupled simulation and the interface pressure calculation models are established with the cast-rolling velocity as the variable. The results show that the interface temperature decreases, the interface pressure and the proportion of the thickness of the Al side increase with the decrease in cast-rolling velocity. The thinning of Cu strip mainly occurs in the backward slip zone. The higher pressure and longer solid/semi-solid contact time make the interface bonded fully, which provides favorable conditions for atomic diffusion. The inter-diffusion zone with a width of 4.9 µm is attained at a cast-rolling velocity of 2.4 m/min, and the Cu side surface is nearly completely covered by aluminum. Therefore, the ductile fracture occurs on the Al side, which prevents the propagation of interface delamination cracks effectively. Meanwhile, shear effect becomes more significant at high interfacial pressure and large plastic strain, and the microstructure on Al side is composed of slender columnar crystals. Thus, the metallurgical bonding and refinement of grains on the Al side can result in higher bonding strength and tensile properties of the clad strip.

Key words: Cu/Al clad strip; cast-rolling velocity; bonding interface; twin-roll casting

## 1 Introduction

Twin-roll casting (TRC) for fabricating bimetal clad materials is a near-end forming process. High temperature and rolling pressure increase the interfacial bonding strength, which improves the performance of clad materials. Compared with those of rolling, the main advantages of TRC are short-flow, energy-saving, and high efficiency [1]. Various products have been successfully prepared by this method to meet the demanding industrial requirements and make economic benefits. Examples are Ti/Al [2], Cu/Al [3], steel/Al [4], Mg/Al [5] clad strips, and bimetallic clad pipes/bars [6], which can combine the excellent properties

of different metals.

Efforts have been made on the research and development of the relationship between process parameters and bonding interface properties. The thermal–force coupling is involved in TRC of bimetal clad strip, which makes the bonding process more complicated. HAGA et al [7] investigated the effect of 3003 substrate strip preheating temperature on the bonding with 4045 overlay strip. The results showed that the shear stress increased with the increase of preheating temperature, cold-rolling could be conducted without peeling and no cracks occurred at the interface when the 3003 strip temperature was in the range from 400 to 550 °C. Similarly, according to the experimental results of CHEN et al [8], the

peeling strength of steel/Al was favorable at high pouring temperature when the cast-rolling velocity was low. The solid/semi-solid contact time was found to be dependent on cast-rolling velocity but directly determined the inter-diffusion zone width. The reasonable structure design and optimization of melt cladding delivery device [9,10] ensure the uniformity of temperature and flow state velocity field in cast-rolling zone, which is beneficial to the atomic diffusion and metallurgical bonding between the bimetallic strips. CHEN and XU [11] studied the effect of melt pressure on bonding strength and process stability of steel/Al clad strip. The results showed that the melt wetting and distribution were more uniform under high melt pressure, and clad strip with intact shape and favorable appearance could be produced. Moreover, the annealing treatment [2,12] on the interface structure, after TRC, is also a key to preparing high-performance clad strip. Thus, the influence of process parameters in the bonding process should be investigated.

To date, most of the studies have focused on the diffusion behavior of the contact interface. The molten metal and solid cladding contact tightly under interface pressure to facilitate diffusion, and the effect of extrusion and crushing makes the components expose fresh metal to participate in bonding. The thickness ratio of substrate to cladding is also different. Previous work showed that such factors as cast-rolling velocity, substrate thickness and material had obvious effects on rolling force [13], which was closely related to the height of kissing point (KP). The KP actually does not exist and is generally considered to be the boundary between solid (semi-solid) and liquid, which is the core of cast-rolling process control. GRYDIN et al [14] qualitatively determined the position of the KP according to the grain size change of liquid aluminum through an emergency stop experiment. STOLBCHENKO et al [15] obtained the KP height and the temperature distribution by establishing a 2D numerical simulation of the steel/aluminum cast-rolling process and analyzed the heat transfer, viscous flow, solidification, and temperature change due to the deformation. LEE et al [16] conducted the thermalfluid-mechanical analysis of twin-roll casting of A7075 aluminum strip by finite element method. Temperature profile, roll separation force, liquid fraction, and metal flow of aluminum strips with different thicknesses were predicted. Consequently, numerical simulation has become one of the useful tools for obtaining the temperature and flow field changes in molten pool.

In this work, industrially pure Al and Cu cladding were taken as the molten substrate strip and cladding metals, respectively. The interface pressure calculation model of clad strip was established and the interfacial pressure distribution on the contact arc was obtained from the numerical simulation results of molten pool temperature field under different cast-rolling velocities. The deformation characteristics of metal component at different cast-rolling velocities and the effects of bonding strength and microstructure of Al on tensile properties were investigated in detail. The mechanism of interface pressure on TRC of bimetal clad strip was discussed as well.

# 2 Experiment and simulation

## 2.1 Experiment

The horizontal TRC process of fabricating bimetallic clad strip has been described in previous reports. As shown in Fig. 1, solid Cu and molten Al are fed into the cast-rolling zone simultaneously, which is formed by side baffle and two rollers. The inner surface of roller sleeve is cooled by cooling water. The combination of rapid solidification and roll bonding technology has enabled the contact interface of metal materials to form a metallurgical bonding under the combined effect of high-temperature diffusion and rolling pressure. Argon or nitrogen is used as shielding gas and clean pretreatment of Cu surface to avoid oxidation. The experimental parameters are shown in Table 1, and

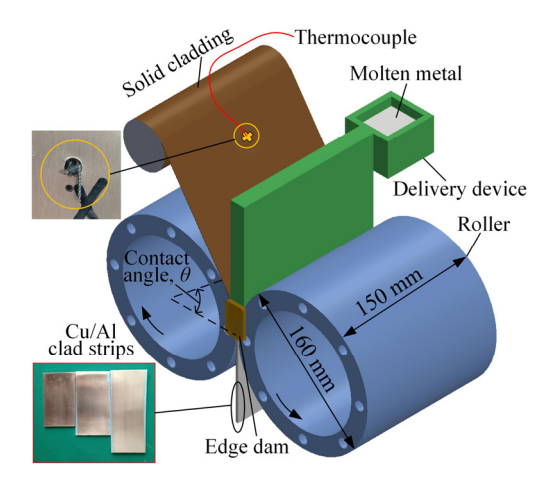


Fig. 1 Schematic diagram of TRC for Cu/Al clad strips

Table 1 Experimental parameters

Parameters	Value	
Casting roller size/mm	<i>d</i> 160 × 150	
Roll gap, H/mm	2.3	
Thickness of copper, $H_{Cu}/mm$	0.5	
Casting temperature, $T_{\text{Casting}}/^{\circ}\text{C}$	700	
Molten pool height, L/mm	30	
Temperature of copper, $T_{\rm Cu}/^{\circ}{\rm C}$	25	
Cast-rolling velocity, v/(m·min <sup>-1</sup> )	2.4, 3.0, 3.6	

Cu/Al clad strip is prepared at different cast-rolling velocities. The material of roller is 42CrMo. A thermocouple is installed on the surface of Cu to verify the simulation results, and it is sufficiently far from the inlet to ensure that the process reaches a stable state. During the interface temperature evolution process, the data are collected by an NI data acquisition system, and a DHDAS data acquisition system shows the rolling force.

Tensile properties and peeling strength are key parameters for the measurements of the bonding quality of bimetallic clad strip. Three samples are cut along the cast-rolling direction according to the GB/T 228.1—2010 (metallic materials tensile testing). The average peeling strength (APS) is tested according to GB2792—1998(test method for peeling strength of pressure-sensitive tape at  $180^{\circ}$  angle). APS is calculated according to the formula: APS=F/W (F is the average peeling force, and W is the bonding width). The shape and size of the sample are shown in Fig. 2. The tensile and peel

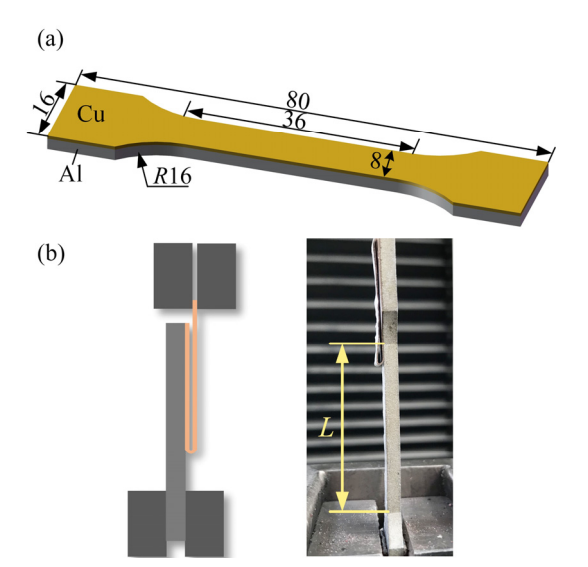


Fig. 2 Schematic diagrams of specimens: (a) Tensile specimen; (b) Peeling specimen (unit: mm)

tests are conducted out using an INSPEKT table 100 kN instrument with the test speed of 5 mm/min. The element distribution across the interface, the morphology of the bonding interface, and tensile fracture are investigated by a scanning electron microscope (SEM-EDS, FEI).

#### 2.2 Simulation

By using FLUENT software, a steady-state thermal-flow coupled simulation model of Cu/Al cast-rolling process is established, including the left roller, molten pool, solid cladding, and right roller. In this simulation, the convective heat transfer coefficient between rollers and cooling water are set to be  $8 \text{ kW/(m}^2 \cdot \text{K})$ . In addition, the interface of two contacting objects is not a perfect-fit state but a discontinuous point contact and contains an air gap. Hence, the interface related to the left roller and right roller is set to be 2 μm, which is of the same order of magnitude as the surface roughness of rollers. From a macroscopic point of view, Al and Cu are bonded well. Thus, the air-gap thickness of Cu/Al is set to to be 0 µm. The thermal conductivity of the air is approximately 0.02 W/(m·K), and the interfacial heat transfer coefficient is 10 kW/(m<sup>2</sup>·K). The specific assumptions and related parameters of simulation model can be referred to Ref. [17], with a very detailed introduction.

Given the small amount of Cu cladding thinning, the deformation of Cu is ignored in this model, and the thickness is 0.5 mm. The outlet thickness of Al is 2 mm. The correctness can be verified by comparing with the interface temperature measurement experiment. Thus, the temperature field and KP height at different cast-rolling velocities are obtained based on the simulation results. Accordingly, the interfacial pressure and the plastic strain of Al can be calculated. Equation (1) [15] is used to calculate the plastic strain:

$$\varepsilon = 1 - \frac{H_{Al}}{H_{Al} + H_{Cu} + 2R - \sqrt{R^2 - l^2} - \sqrt{(R + H_{Cu})^2 - l^2}}$$
(1)

where  $\varepsilon$  is the plastic strain of Al substrate,  $H_{\text{Al}}$  is the thickness of Al substrate,  $H_{\text{Cu}}$  is the thickness of Cu cladding, R is roller radius, and l is the KP height that is the height difference between the KP and the cast-rolling zone outlet.

# 3 Results and discussion

#### 3.1 Temperature field

Figure 3 shows the effect of cast-rolling velocity on the temperature field when  $T_{\text{Casting}}$ = 700 °C and  $H_{\text{Cu}}$ =0.5 mm, which indicates that KP migrates toward the outlet and the outlet temperature increases significantly with the rise in cast-rolling velocity. Thus, the plastic strain of Al decreases, as shown in Fig. 4(a). The cast-rolling zone has three physical states on the Al side: liquid, semi-solid, and solid zones. The semi-solid zone is the area where the metal Al transitions from a complete liquid state to a complete solid state. The deformation resistance of liquid zone is small at high temperatures. Thus, the deformation can be considered to occur only in the semi-solid and solid zones, and the temperature at KP is 660 °C [17]. As casting temperature is kept constant, increasing the velocity enhances the heat input per unit time. As a result, the heat taken away by cooling rollers is reduced due to the decrement in cooling time. When the KP position is too high, continuous production will be disrupted, which will cause rolling stop, and wrinkle the surface of the strip. When the KP position is too low, the liquid Al cannot even be completely filled with the cast-rolling zone or fully solidified, which results in pits on the surface of strip and reduction in bonding strength [8]. Notably, the molten pool temperature is asymmetrically distributed, and the KP has a tendency to migrate to the left roll. This finding indicates that the geometric asymmetry causes asymmetric heat transfer. As shown in Fig. 4(b), the solidified shell thickness evolution is the same at different cast-rolling velocities. The thickness of solidified shell on the Cu cladding side is thicker owing to the favorable thermal conductivity of Cu cladding.

Simulation and experimental results for the interface temperature are given in Fig. 5. The simulation result is consistent with the experimental evolution at 3.6 m/min, which implies that the numerical model is referential. Before and in the cast-rolling zone, the interface temperature increases firstly and then decreases. The difference in outlet temperature is approximately 40 °C. The increase in the cast-rolling velocity increases the maximum and outlet temperature and is labeled in Fig. 5. Comparing experimental result with simulation result shows that the maximum temperature deviation is 90 °C, and the outlet temperature deviation is 74 °C. Thermocouple has a certain volume and hysteresis in temperature test. After leaving the cast-rolling zone, thermocouple temperature increases be consistent with the interface temperature. In air cooling, the interface temperature deviation is 139 °C. Therefore, the instantaneous response deviation of thermocouple at high temperature is approximately 100 °C. The experimental process does not reach a quasi-static state due to the restriction of experimental conditions, such as the fluctuation and height change of the liquid level, which cause test errors. If these interference factors

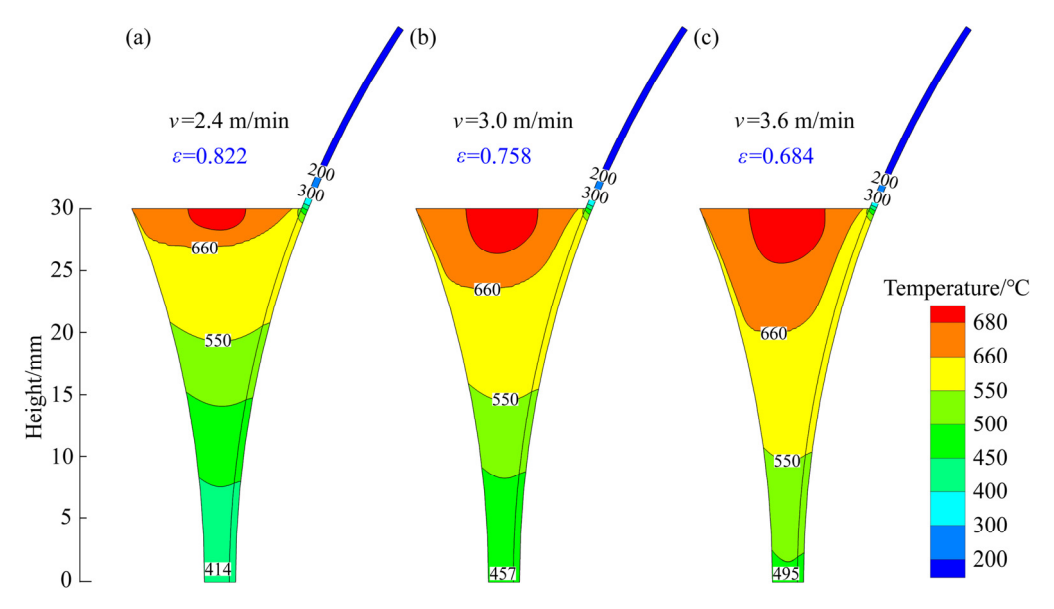


Fig. 3 Temperature field of cast-rolling zone at different cast-rolling velocities when  $T_{\text{Casting}}$ =700 °C and  $H_{\text{Cu}}$ =0.5 mm

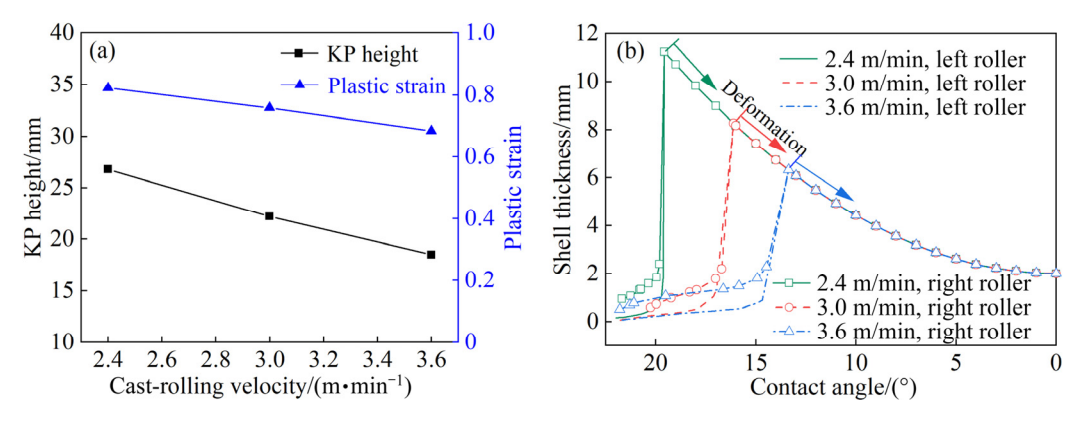
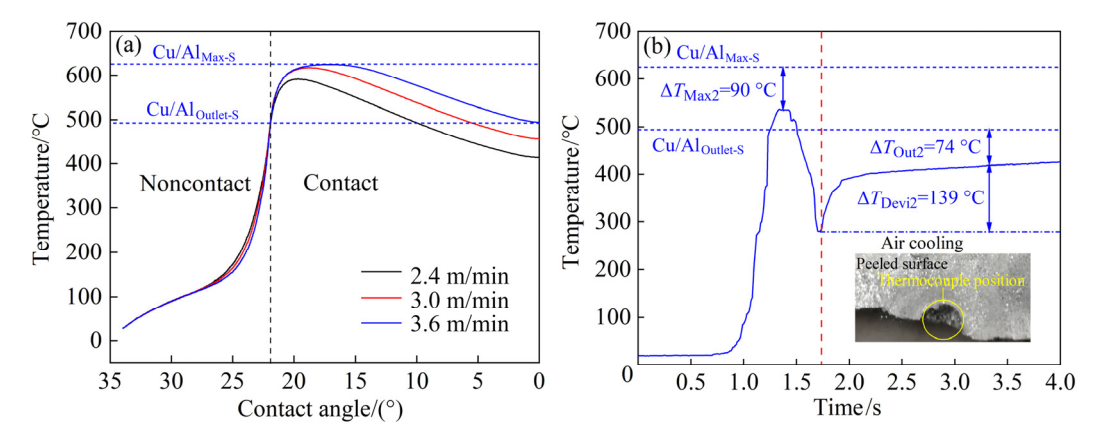


Fig. 4 KP height and plastic strain (a) and shell thickness (b) of Al



**Fig. 5** Interface temperature: (a) Simulation results at different cast-rolling velocities; (b) Experimental results at 3.6 m/min

are considered, the simulation results will agree well with the experimental results.

#### 3.2 Interfacial pressure distribution

For the TRC process, the yield strength along the rolling direction varies greatly owing to the different physical states of molten metal in the cast-rolling process. As a result, the interfacial pressure is difficult to calculate. As shown in Fig. 4(b), the thickness of solidified shell is less than 3 mm. When the interfacial pressure distribution on the contact arc of Cu/Al clad strip is calculated, the hot rolling deformation of the solid—solid strip can be approximately considered under the KP. The deformation of Al satisfies von Mises yield criterion under the condition of plane plastic deformation. Slip friction is considered in the deformation zone, and the cladding and substrate strip are bonded at the outlet.

Figure 6 shows the geometric parameters of cast-rolling zone and the element stress analysis, where x is the element height,  $h_x$  is the element

thickness,  $h_0$  is the thickness of Al at KP, h is the outlet thickness of Al,  $\Delta h$  is the plastic strain, and  $\alpha$  is the contact angle. There are the following geometric relations according to the thickness evolution of the Al during deformation:

$$h_x = 2(R - \sqrt{R^2 - x^2}) + h \tag{2}$$

$$\alpha = \arccos \frac{2R - (h_x - h)}{2R} \tag{3}$$

The equilibrium differential equation is obtained along the rolling direction by taking a micro element in the backward slip zone for stress analysis:

$$2(\sigma_x + d\sigma_x) \left( \frac{h_x}{2} + d\left(\frac{h_x}{2}\right) \right) - 2\sigma_x \frac{h_x}{2} - 2p \tan \alpha dx + 2\tau dx = 0$$
(4)

where  $\sigma_x$  is the stress, p is the unit pressure and  $\tau$  is tangential stress.

Take  $\tan \alpha = [d(h_x/2)]/dx$  into Eq. (4), and the higher-order terms are removed to obtain the following equation:

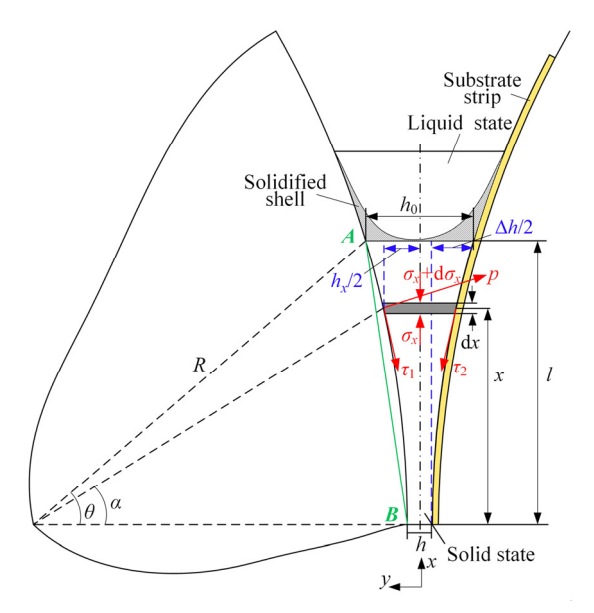


Fig. 6 Schematic diagram for stress analysis of micro element in deformation zone

$$\frac{\mathrm{d}\sigma_x}{\mathrm{d}x} - \frac{p - \sigma_x}{y} \frac{\mathrm{d}(h_x/2)}{\mathrm{d}x} + \frac{\tau}{(h_x/2)} = 0 \tag{5}$$

The frictional forces ( $\tau_1$  and  $\tau_2$ ) on both sides of Al are as follows:  $\tau_1 = \mu_1 p$ ,  $\tau_2 = \mu_2 p$ , and friction coefficients  $\mu_1 = 0.4$  and  $\mu_2 = 0.27$  [13].

During the TRC process, the shearing deformation work theory, as a yield condition of the material [18], is approximately expressed as

$$p - \sigma_x = K$$
 (6)

$$dp = d\sigma_x$$
 (7)

where *K* is the deformation resistance of Al. According to the research of ZHAN [19] on the rheological behavior of industrial pure Al at high temperature, the plane deformation resistance of Al decreases with the increase in temperature. Thus, the deformation resistance of pure Al at different temperatures is obtained, as shown in Fig. 7(a). The

deformation resistance is nearly 7.5 MPa at 660 °C. Simulation results of temperature field are used as a reference to determine the specific values.

To simplify the calculation, the corresponding contact arc is replaced by a string. The linear equation of string AB is

$$\frac{h_x}{2} = \frac{\Delta h}{2l} x + \frac{h}{2} \tag{8}$$

After derivation, we have

$$dx = \frac{2l}{\Delta h} d\left(\frac{h_x}{2}\right) \tag{9}$$

When the tension  $\sigma_0$  is applied, the initial condition is the entrance:

$$\begin{cases} y = \frac{h_0}{2} \\ p = K - \sigma_0 = K(1 - \frac{\sigma_0}{K}) = \varepsilon_0 K \\ \varepsilon_0 = 1 - \frac{\sigma_0}{K} \end{cases}$$
 (10)

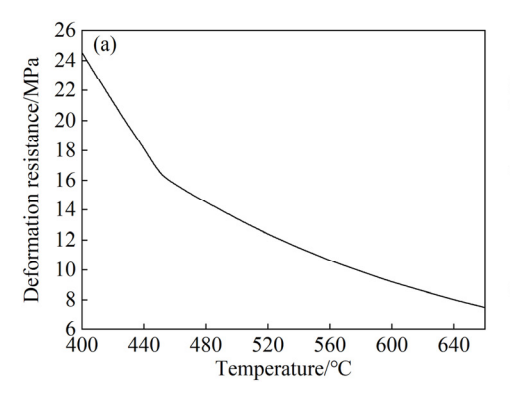
By integrating Eq. (5) and let  $\delta = (2l\mu)/\Delta h$ , the contact normal stress of each micro element in the backward slip zone without tension can be obtained as follows:

$$p = \frac{K}{\delta} \left[ (\delta - 1) \left( \frac{h_0}{h_x} \right)^{\delta} + 1 \right]$$
 (11)

Similarly, the contact normal stress of each micro element in the forward slip zone without tension can be obtained as follows:

$$p = \frac{K}{\delta} \left[ (\delta + 1) \left( h_x / h \right)^{\delta} - 1 \right]$$
 (12)

In the calculation, the entrance contact arc  $\theta$  of the deformation zone is divided into m equal parts. Contact pressure of the backward and the forward slip zones can be calculated alternately.



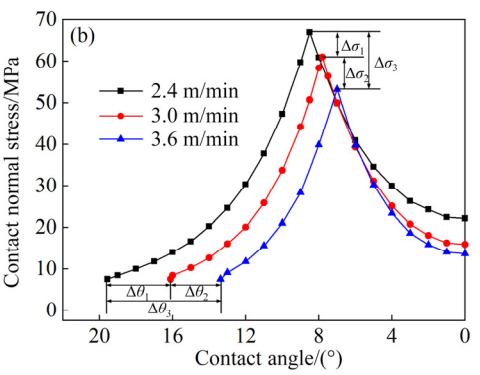


Fig. 7 Deformation resistance of Al (a) and interfacial pressure distribution (b)

When the contact normal stress of the backward slip zone is greater than that of the forward slip zone, the calculation of the forward slip zone begins; otherwise, the calculation of the backward slip zone continues. When the calculated values of both sides are equal, the contact angle at the neutral point is the neutral angle. Figure 7(b) shows the calculation results of contact normal stress. The results indicate that the interfacial pressure presents a unimodal shape in the whole deformation zone. The contact normal stress increases gradually from the KP along the rolling direction, reaches the maximum at neutral point, and then decreases. With the increase in cast-rolling velocity, the position of neutral point migrates to the outlet, and the maximum stress decreases owing to the overall increase in temperature and the decrease in deformation resistance.

The total rolling force is the sum of the force of the substrate strip and cladding in TRC process for bimetallic clad strip. The rolling force of Al side can be calculated by Eqs. (13) and (14). For example, the calculated rolling force of Al side is 92 kN when the cast-rolling velocity is 3.6 m/min. Repeated simulation is conducted on the TRC of single Al. The KP height at the cast-rolling velocity of 2.5 m/min is close to that in Fig. 3(c) under the same conditions. The measured rolling force is 100 kN at 2.5 m/min for single Al, which is similar to the calculation. This similarity implies that the model has a certain reference value.

$$F = B \frac{\int_0^l p(\cos \alpha + \mu \sin \alpha)}{\cos \alpha} dx = B \int_0^\theta p(\cos \alpha + \mu \sin \alpha) R d\alpha$$
 (13)

$$F = BR \sum_{n=1}^{\infty} \int_{a_{n}}^{a_{n+1}} p(\cos \alpha \pm \mu \sin \alpha) d\alpha$$
 (14)

where F is the rolling force of Al side, B is the width of cladding strip, m is the number of micro elements,  $\alpha_{n+1}$  and  $\alpha_n$  are angles corresponding to both sides of the element. The backward slip zone is "+" and the forward slip zone is "–".

The rolling force decreases with the increase in cast-rolling velocity, and it affects the final component thickness ratio and bonding quality of products. Figure 8(a) shows the measured results at different cast-rolling velocities. As observed, the rolling force decreases with the increase in castrolling velocity, and it is 130 kN at 3.6 m/min. A slice sample at v=2.4 m/min is cut through emergency stop and quick cooling. Figure 8(b) shows the macroscopic evolution of the bonding interface in cast-rolling zone. A gap exists near the inlet of the rolling zone (Zone I) owing to the small contact pressure between liquid Al and solid Cu. In the contact moment, liquid Al forms a solidified shell rapidly. Consequently, fresh metal should be exposed under pressure extrusion to participate in bonding for achieving the effective bonding interface. Below the KP, mechanical occlusion and element diffusion promote metallurgical bonding. Cu cladding has obvious thinning process in Zone II, from 0.46 to 0.44 mm, but small cracks are still present. The interface is well bonded near the outlet (Zone III).

Figure 9(a) shows the thickness evolution of Cu cladding throughout the slice sample. With the rolling process, the thickness of Cu cladding changes from 0.5 to 0.2 mm, and the thinning can be divided into three parts. The small thinning in

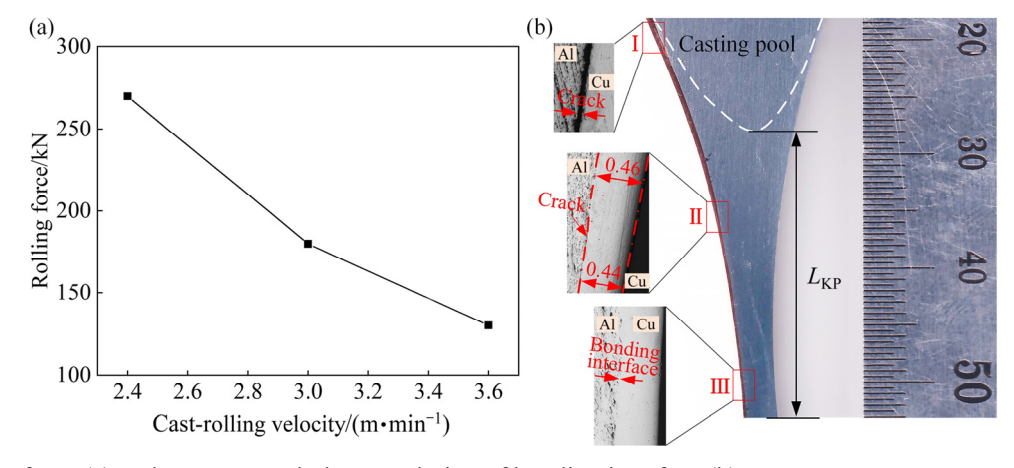


Fig. 8 Rolling force (a) and macro-morphology evolution of bonding interface (b)

liquid zone supports the rationality of ignoring the effect of liquid zone when calculating the interface pressure. Cu cladding thinning occurs mainly in the backward slip zone, and the thickness remains unchanged after a small thinning in the forward slip zone. As shown in Fig. 9(b), the thickness ratio of Al substrate to Cu cladding is different. With the increase in velocity, the thinning amount of Cu decreases, and the thickness proportion ( $\lambda$ ) of Al decreases. LIU et al [20] emphasized that contact time of liquid and solid is an important factor, and short time is unfavorable. Thus, the main effect is the contact time between the solid/semi-solid Al and the solid Cu, that is, the section below KP. As shown in Fig. 9(b), the time is less than 1 s. Comparing the contact time with the diffusion zone thickness introduced in this work indicates that both evolutions are consistent, and the diffusion zone is wider when the time is longer.

# 3.3 Bonding interface morphology and diffusion

Figure 10 shows the SEM images and typical elemental distributions for bonding interface of Cu/Al clad strip at different cast-rolling velocities. No obvious holes are observed, and the large plastic deformation results in the wavy interface. Intuitively, the diffusion layer is the thickest at 2.4 m/min and slight crack is observed at 3.6 m/min at the interface, which means that the wetting and distribution of molten Al on the solid Cu surface are uneven at low pressure.

The typical elemental distributions across the interface show that thicknesses of the interdiffusion layer of Cu and Al decrease with the

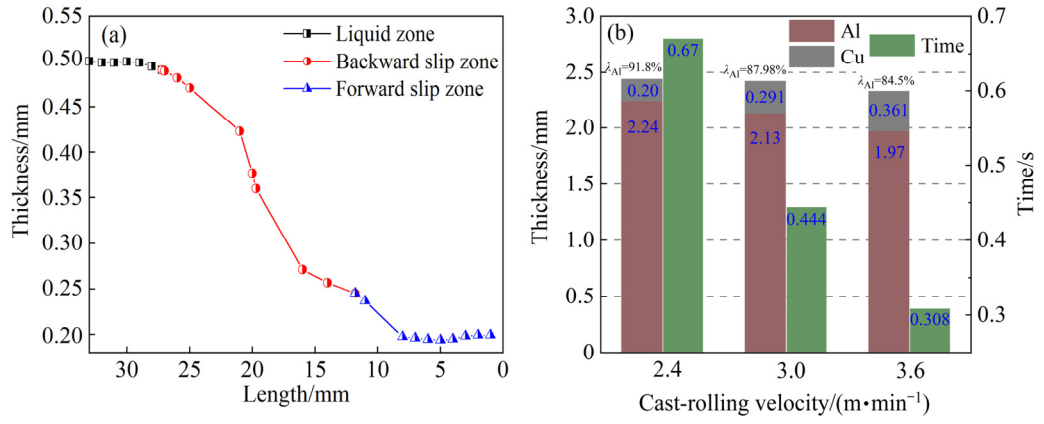
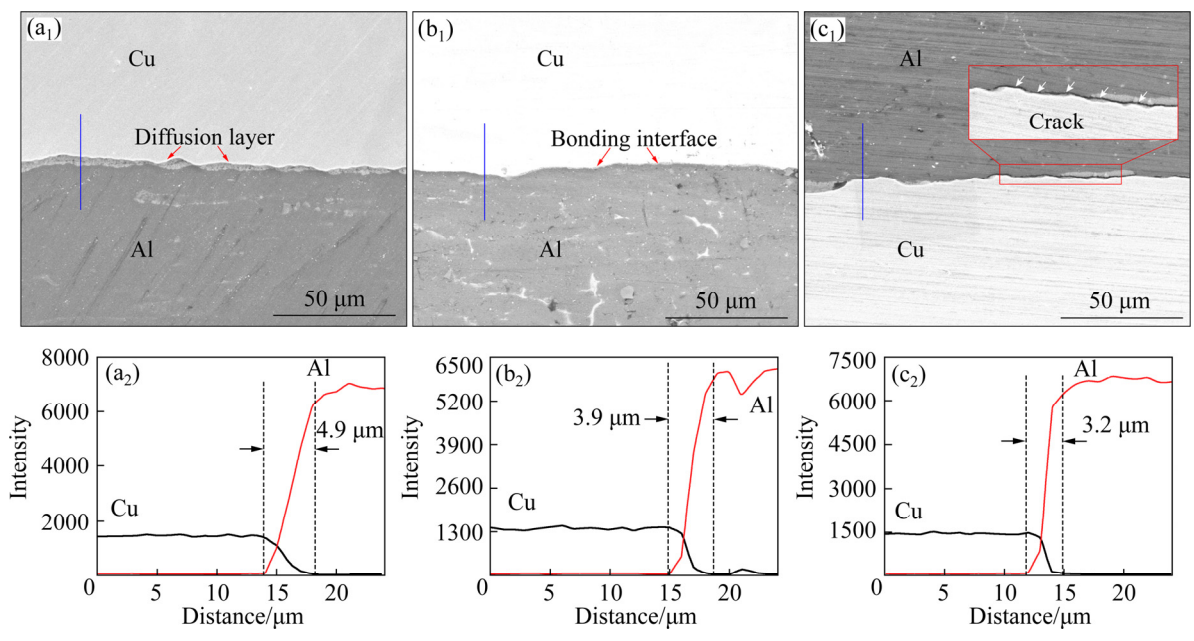


Fig. 9 Cu strip thickness evolution (a), component thickness and rolling time in deformation zone (b)



**Fig. 10** SEM images  $(a_1, b_1, c_1)$  and typical elemental distributions of bonding interface  $(a_2, b_2, c_2)$ :  $(a_1, a_2)$  v=2.4 m/min;  $(b_1, b_2)$  v=3.0 m/min;  $(c_1, c_2)$  v=3.6 m/min

increase in cast-rolling velocity. The migration ability of metal atoms will become increasingly stronger with the rise in the rolling temperature. Interestingly, the increase in cast-rolling velocity increases the interface temperature but decreases diffusion thickness of layer. Previous investigations found that the mutual diffusion was promoted by plastic deformation through three basic mechanisms: induced atomic displacements, pipe diffusion along dislocations, and plastic deformation induced vacancies [21,22]. However, dislocations caused by plastic deformation were mainly distributed at grain boundaries [23], and atomic migration was difficult. On the crystal defects, the vacancy caused by plastic deformation has low migration energy [24] and promotes the diffusion of atoms, which is related to the interface pressure. Therefore, high interfacial contact pressure should be of primary importance in addition to increasing the casting temperature for improving the bimetallic bonding properties in TRC.

#### 3.4 Micromorphology of peeled surface

Figure 11 shows the average peeling strength (APS) of samples at different cast-rolling velocities. The results show that APS decreases with the increase in velocity. According to LIU et al [25], the bonding interface in the clad strip can be solid solution strengthened by the inter-diffusion effect, and the strengthening effect is stronger when the inter-diffusion zone is larger. Thus, low interfacial pressure, short contact time, and uneven wetting at 3.6 m/min make the peeling strength decrease. The annealing of cast-rolling clad strip shows that the thickness of interfacial diffusion layer continues to

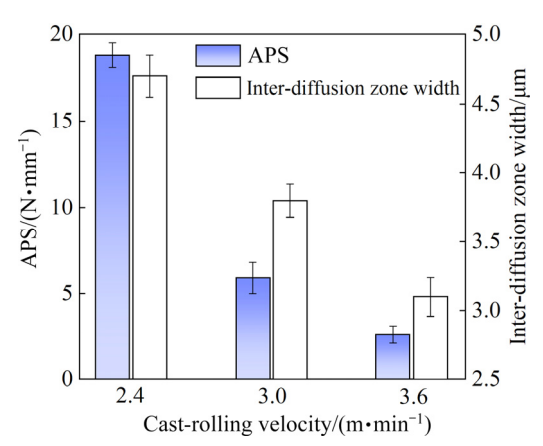


Fig. 11 Average peeling strength (APS) and width of inter-diffusion zone at different cast-rolling velocities

increase with the rise in annealing temperature, while the peeling strength increases firstly and then decreases [2,26]. Thus, the bonding strength of Cu/Al clad strip prepared by TRC can still be improved.

12 shows the peeled surface morphologies of Cu/Al clad strip at different cast-rolling velocities. The peeled surface on the Cu and Al sides is in convex ridge-shape at 2.4 m/min. During the peeling process, Al undergoes large plastic deformation and gradually tears and adheres to the copper tape after reaching the breaking strength. This form is a typical ductile fracture characteristic. At 3.0 m/min, the peeling surface is discontinuous flat block. Similarly, the peeling surface is flat and many scattered pits appear at 3.6 m/min. Both are brittle fractures. The SEM-EDS mapping images and element contents of Cu side are shown in Fig. 13, which confirms that the fracture occurs on the Al side. The contents of Al element are 54 at.%, 33 at.%, and 29 at.%. With the increase in cast-rolling velocity, the fracture mode of the peeling surface changes from ductile fracture to brittle fracture. The above mentioned analysis shows that the Cu/Al clad strip has good bonding performance under the action of higher interface pressure and longer contact time.

The compounds include Cu<sub>9</sub>Al<sub>4</sub>, CuAl<sub>2</sub>, and CuAl at the composite interface of Cu/Al clad strip prepared by TRC [3,12], and the content decreases sequentially. The EDS spectra of Spots 1–11 in Fig. 12 are analyzed to study the influence of interface products on bonding strength. Table 2 shows the element contents. The compound can be inferred based on the element content ratio, and the results show that the interface compound types are the same. Thus, the thickness of interface diffusion layer directly affects the bonding strength. However, the diffusion layer is inherently brittle. Therefore, the thickness must be reasonably controlled.

#### 3.5 Tensile properties

Figure 14 shows the tensile engineering stress—strain curves of Cu/Al clad strip at different cast-rolling velocities. Bimetallic stretching forms synergistic deformation followed by the occurrence of necking, because the elongation of Cu cladding is smaller than that of Al, resulting in the fracture in the necking area successively. With the increase in cast-rolling velocity, the yield strength, tensile

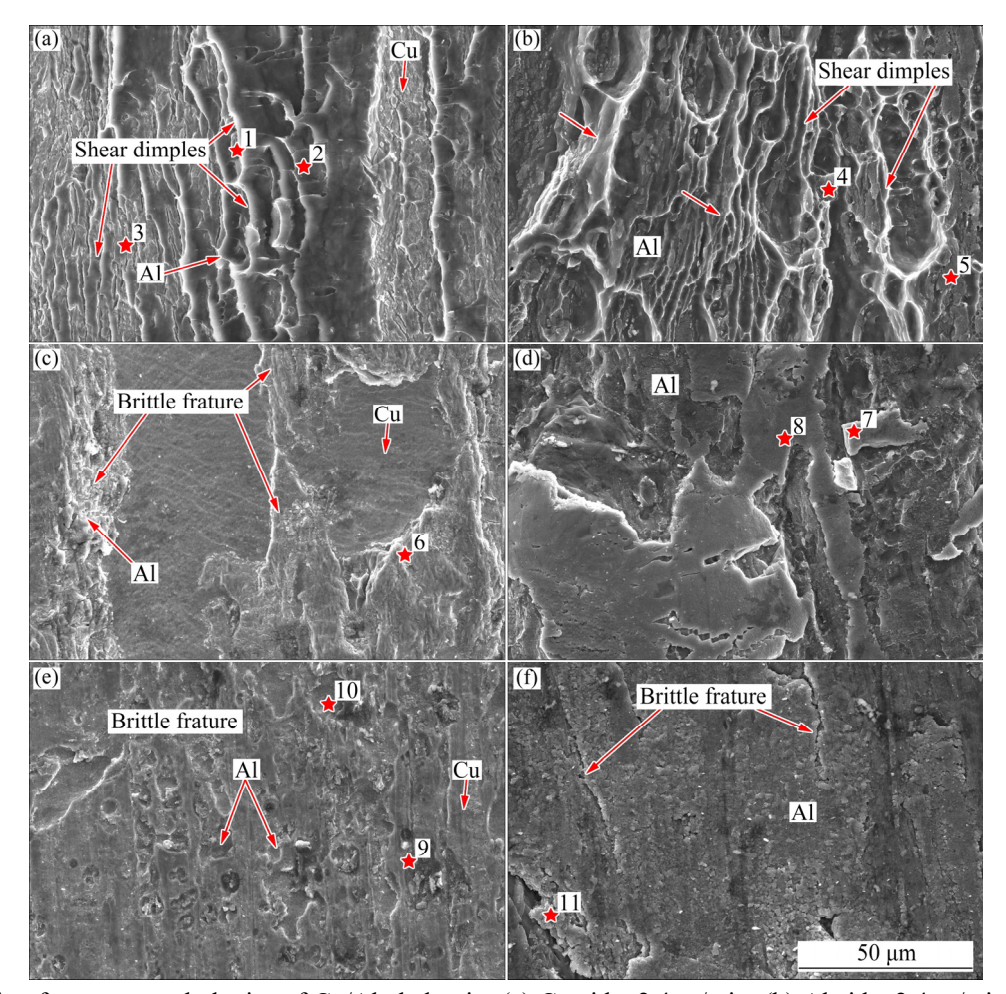


**Fig. 12** Peeling fracture morphologies of Cu/Al clad strip: (a) Cu aide, 2.4 m/min; (b) Al side, 2.4 m/min; (c) Cu aide, 3.0 m/min; (d) Al side, 3.0 m/min; (e) Cu side, 3.6 m/min; (f) Al side, 3.6 m/min

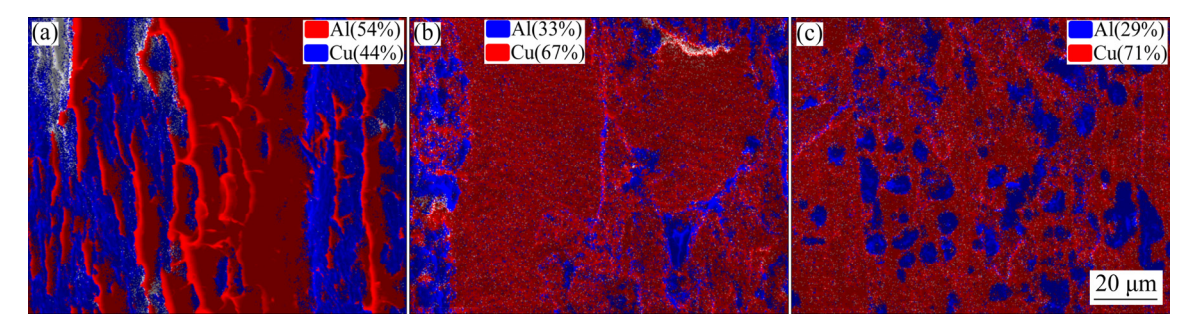


**Fig. 13** SEM-EDS mapping images and element contents on Cu side at different cast-rolling velocities: (a) 2.4 m/min; (b) 3.0 m/min; (c) 3.6 m/min

strength, and elongation decrease gradually. The ultimate tensile strength of Cu/Al clad strip is obviously higher than that of single Al in Figs. 14(a) and (c), which implies that the combination of Al and Cu could enhance the strength. Notably, the elongation is also enhanced, because the mutual restraint between adjacent layers of metal will cause the inhibition of local deformation and the formation of diffusion layer will reduce the fracture

strain [27].

The side view shape of the tensile fracture differs with different bonding strengths of bimetallic clad strip. Figure 15 shows the profile revealing tensile fracture characteristics of Cu/Al clad strip at different cast-rolling velocities. After fracture, the interface is still tightly bonded at 2.4 m/min, and the fracture presents symmetrical necking. A high interfacial bonding strength can

Table 2 EDS results of Spots 1-11 in Fig. 12

Table 2 LDS results of Spots 1 11 m 11g. 12			
Point No.	Al content/at.%	Cu content/at.%	Phase
1	66.83	33.17	AlCu
2	68.99	32.01	Al <sub>2</sub> Cu
3	25.25	74.75	Al <sub>4</sub> Cu <sub>9</sub>
4	68.86	31.14	$Al_2Cu$
5	67.54	32.46	Al <sub>2</sub> Cu
6	23.90	76.10	Al <sub>4</sub> Cu <sub>9</sub>
7	64.29	35.71	$Al_2Cu$
8	52.22	47.78	AlCu
9	54.27	45.73	AlCu
10	28.18	71.82	Al <sub>4</sub> Cu <sub>9</sub>
11	66.06	33.94	Al <sub>2</sub> Cu

withstand large normal and shear forces, and this feature hinders the propagation of delamination cracks. Thus, the first fracture in the tensile curve is not obvious. Figure 15(b) shows the bonding interface. The fracture surfaces of the Al side are all dimpled, which shows typical ductile fracture characteristics. The decrease in bonding strength leads to the fracture of the interface at 3.0 m/min,

and the situation is similar at 3.6 m/min but the length of interfacial delamination is longer. Therefore, Al will stretch a small length alone in the tensile process. In summary, the strong interfacial bonding performance positively affects the prevention of interfacial separation in the tensile process [28].

For bimetallic clad strip, the accumulation of dislocation density caused by large plastic strain leads to the work hardening. This phenomenon increases the yield strength and tensile strength but reduces the elongation. The grain refinement by appropriate annealing [29] and asymmetric rolling [30] can improve the ductility [31]. Notably, the microstructure of Al in Cu/Al clad strip has a great influence on the total elongation. The microstructures of Al at different cast-rolling velocities are obtained by mechanical polishing, electropolishing, and anodizing, and the results are shown in Fig. 16. Plastic shear occurs in the solidification process of liquid Al, and the shear effect of plastic strain and interfacial pressure at low cast-rolling velocity is more significant. The results indicate that the grain structure consists of slender columnar grain at 2.4 m/min, and the situation is similar at 3.0 m/min. Meanwhile, the

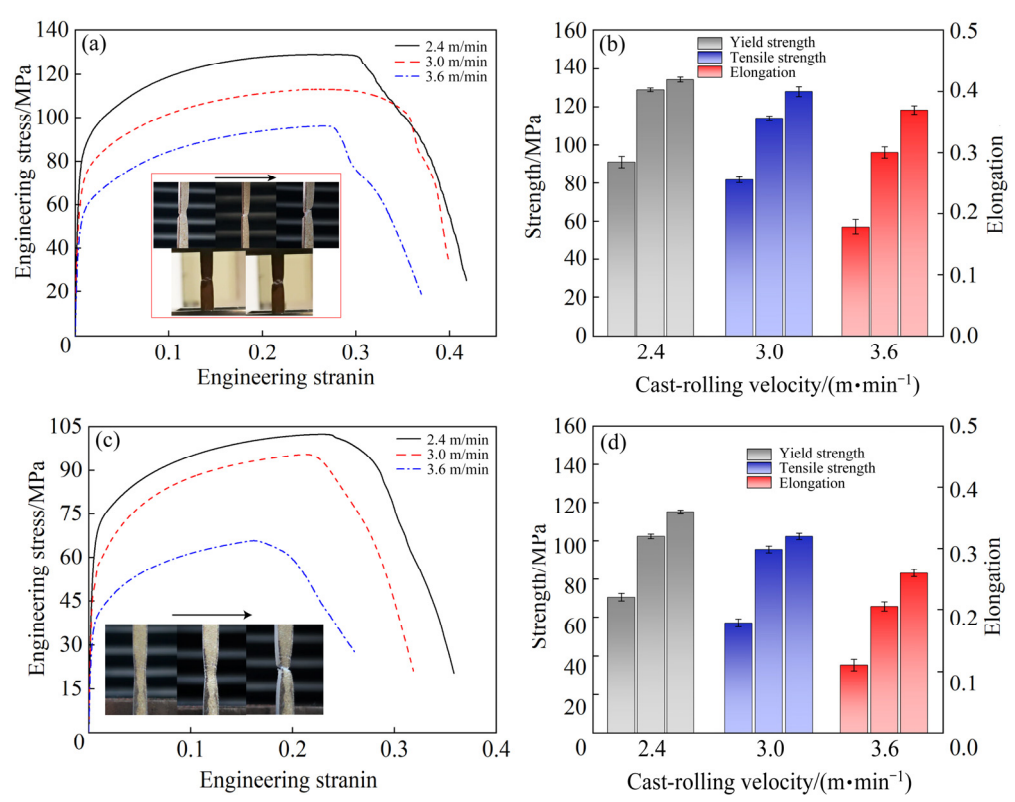
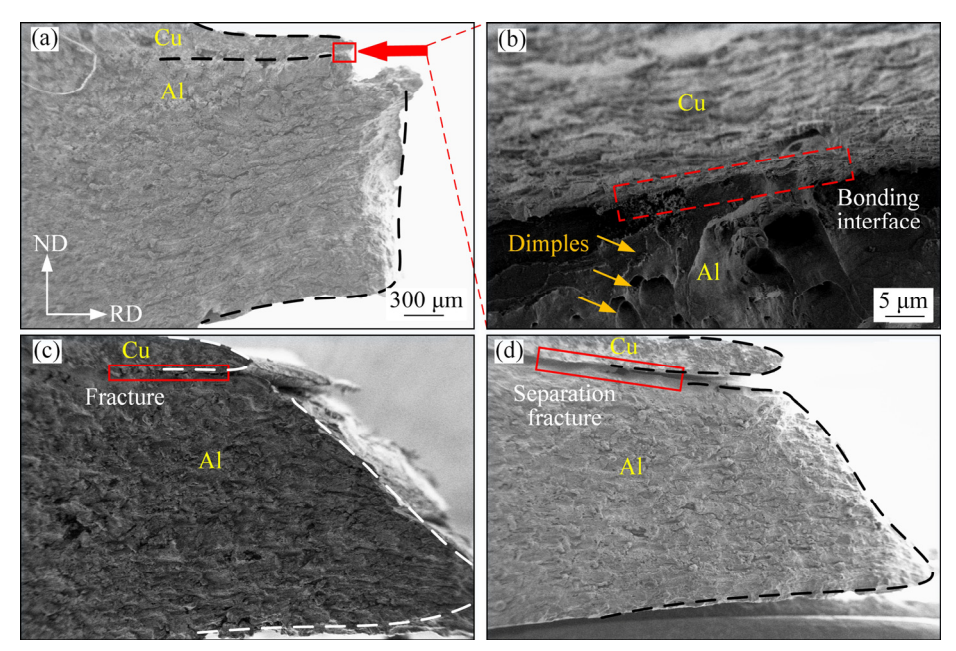


Fig. 14 Engineering stress-strain curves and tensile properties at different cast-rolling velocity: (a, b) Cu/Al clad strip; (c, d) Al



**Fig. 15** Tensile fracture side view morphologies: (a) v=2.4 m/min; (b) Enlarged view of bonding interface in (a); (c) v=3.0 m/min; (d) v=3.6 m/min

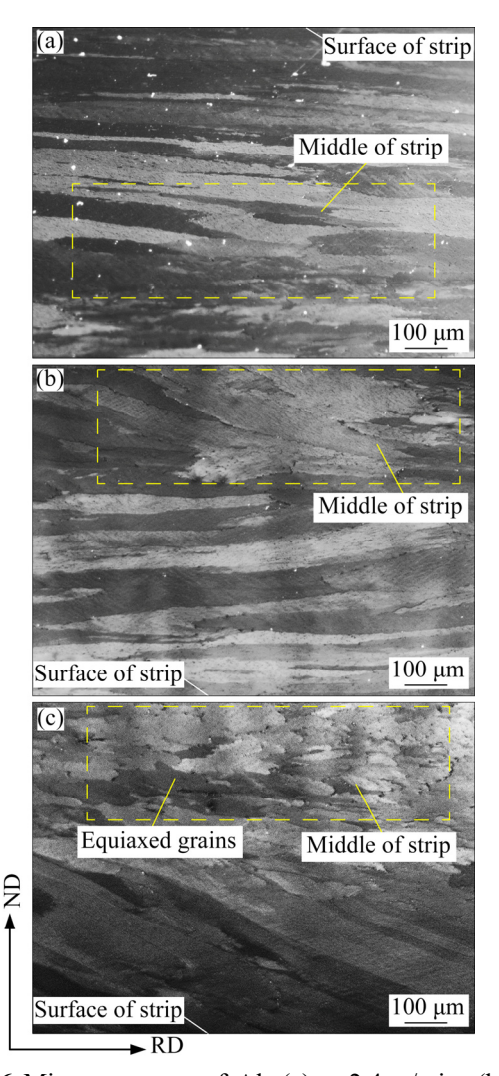


Fig. 16 Microstructures of Al: (a) v=2.4 m/min; (b) v=3.0 m/min; (c) v=3.6 m/min

grain size increases especially in the core. When the velocity is 3.6 m/min, the grain size continues to increase near the surface of the strip. The high temperature and short shear deformation time cause obvious segregation surface and equiaxed crystal in the core of Al, which is the solidification structure without plastic deformation [32]. Inclined bands near the surface of the strips indicate the plastic strain during the TRC. As a result, the elongation performance of the Cu/Al strip and single Al after peeling at 2.4 m/min is better due to the refined grains.

In summary, the bonding strength and grain structure of Al determine the tensile strength and tensile elongation of Cu/Al clad strip, respectively, as shown in Fig. 17. The same is true for other bimetallic clad strips. Notably, interface pressure is the guarantee of full infiltration, and it also determines the thickness ratio of the product.

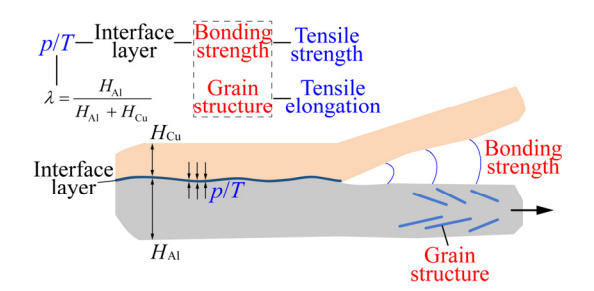


Fig. 17 Diagram of tensile property strengthening mechanism

## **4 Conclusions**

- (1) Increasing the cast-rolling velocity enhances the heat input per unit time, the KP migrates toward the outlet, and the bonding interface temperature increases significantly as casting temperature is kept constant.
- (2) The interfacial pressure should be of primary importance in addition to the casting temperature and presents a unimodal shape. Cu cladding thinning occurs mainly in the backward slip zone. With the increase in cast-rolling velocity, the position of neutral point migrates to the outlet, and the maximum interfacial stress decreases. As a result, the thinning amount of Cu and the thickness proportion of Al decrease.
- (3) The higher pressure and longer solid/semi-solid contact time make the interface bonded fully, which provides favorable conditions for the atomic diffusion. It also prevents the propagation of interface delamination cracks effectively. A wide zone of 4.9  $\mu$ m is attained under condition of cast-rolling velocity of 2.4 m/min, and the Cu side surface is by aluminum. Therefore, the ductile fracture occurs on the Al side.
- (4) The ultimate tensile strength and elongation of Cu/Al clad strip in TRC depend on bonding strength and grain structure of Al, and the combination of Al and Cu could enhance the strength. The shear effect of plastic strain and interfacial pressure at low cast-rolling velocity is more significant, which can refine the grain and improve elongation.

#### **Acknowledgments**

The authors are grateful for the financial support from the National Natural Science Foundation of China (No. 51974278), the Natural Science Foundation of Hebei Province Distinguished Young Fund Project, China (No. E2018203446), and the National Foundation of Key Research and Development Project of China (No. 2018YFA0707303).

# References

 KUMAI S, TAKAYAMA Y, NAKAMURA R, SHIMOSAKA D, HARADA Y, KIM M S. Application of vertical-type high-speed twin-roll casting for up-grade recycling and clad sheets fabrication of aluminum alloys [J]. Materials Science

- Forum, 2016, 877: 56-61.
- [2] HUANG Hua-gui, CHEN Peng, JI Ce. Solid-liquid cast-rolling bonding (SLCRB) and annealing of Ti/Al cladding strip [J]. Materials & Design, 2017, 118: 233–244.
- [3] HUANG Hua-gui, DONG Yi-kang, YAN Meng, DU Feng-shan. Evolution of bonding interface in solid-liquid cast-rolling bonding of Cu/Al clad strip [J]. Transactions of Nonferrous Metals Society of China, 2017, 27(5): 1019–1025.
- [4] GRYDIN O, GERSTEIN G, NURNBERGER F, SCHAPER M, DANCHENKO V. Twin-roll casting of aluminum-steel clad strips [J]. Journal of Manufacturing Processes, 2013, 15(4): 501-507.
- [5] BAE J H, PRASADA RAO A K, KIM K H, KIM N J. Cladding of Mg alloy with Al by twin-roll casting [J]. Scripta Materialia, 2011, 64(9): 836–839.
- [6] JI Ce, HUANG Hua-gui, SUN Jing-na, CHEN Peng. Process window prediction of solid-liquid cast-rolling bonding (SLCRB) process through numerical analysis to fabricate bimetallic clad pipes [J]. International Journal of Heat and Mass Transfer, 2018, 120: 1305–1314.
- [7] HAGA T, OKAMURA K, WARARI H, NISHIDA S. Effect of base strip temperature on bonding of three-layer clad strip cast by a vertical-type tandem twin roll caster [J]. Key Engineering Materials, 2018, 792: 8–15.
- [8] CHEN Gang, LI Jin-tao, XU Guang-ming. Bonding process and interfacial reaction in horizontal twin-roll casting of steel/aluminum clad sheet [J]. Journal of Materials Processing Technology, 2017, 246: 1–12.
- [9] CHEN Yao, WANG Ai-qing, TIAN Han-wei, XIE Jing-pei, WANG Xiang. Study on optimization of nozzle for copper-aluminium clad plate twin-roll cast-rolling [J]. Journal of Materials Research and Technology, 2021, 10(4): 1075-1085.
- [10] HUANG Hua-gui, JI Ce, YANG Zhi-qiang, YAN Meng. Implementation and forming mechanism of the solid-liquid cast-rolling bonding (SLCRB) process for steel/Al clad pipes [J]. Journal of Manufacturing Processes, 2017, 30: 343–352.
- [11] CHEN Gang, XU Guang-ming. Effects of melt pressure on process stability and bonding strength of twin-roll cast steel/aluminum clad sheet [J]. Journal of Manufacturing Processes, 2017, 29: 438–446.
- [12] MAO Zhi-ping, XIE Jing-pei, WANG Ai-qing, WANG Wen-yan, MA Dou-qin, LIU Pei. Effects of annealing temperature on the interfacial microstructure and bonding strength of Cu/Al clad sheets produced by twin-roll casting and rolling [J]. Journal of Materials Processing Technology, 2020, 285: 116804–116812.
- [13] ZHANG Jun-peng, HUANG Hua-gui, ZHAO Ri-dong, FENG Miao, MENG Kai. Cast-rolling force model in solid-liquid cast-rolling bonding (SLCRB) process for fabricating bimetal clad strips [J]. Transactions of Nonferrous Metals Society of China, 2021, 31(3): 626-635.
- [14] GRYDIN O, STOLBCHENKO M, SCHAPER M. Deformation zone length and plastic strain in twin-roll casting of strips of Al–Mg–Si alloy [J]. JOM, 2017, 69(12): 2648–2652.
- [15] STOLBCHENKO M, GRYDIN O, SAMSONENKO A, KHVIST V, SCHAPER M. Numerical analysis of the twinroll casting of thin aluminium-steel clad strips [J]. Forschung Ingenieurwes, 2014, 78(3/4): 121-130.

- [16] LEE Y S, KIM H W, CHO J H, CHUN S H. Coupled thermal-fluid-mechanics analysis of twin roll casting of A7075 aluminum alloy [J]. Metals and Materials International, 2017, 23(5): 923–929.
- [17] JI Ce, HUANG Hua-gui, ZHANG Jun-peng, ZHAO Ri-dong. Influence of the substrate strip on the asymmetric heat transfer of twin-roll casting for fabricating bimetallic clad strips [J]. Applied Thermal Engineering, 2019, 158: 113818–113829.
- [18] CHEN Shui-xuan, LI Wei-gang, LIU Xiang-hua. Calculation of rolling pressure distribution and force based on improved Karman equation for hot strip mill [J]. International Journal of Mechanical Sciences, 2014, 89: 256–263.
- [19] ZHAN Li-hua. Experimental study on high temperature rheological behavior of commercial pure aluminum [J]. Hot Working Technology, 2006, 35(8): 7–11. (in Chinese)
- [20] LIU Yao-hui, LIU Hai-feng, YU Si-rong. Study on bimetal composite material interface by liquid-solid bonding [J]. Chinese Journal of Mechanical Engineering, 2000, 36(7): 81–85. (in Chinese)
- [21] SAUVAGE X, DINDA G P, WILDE G. Non-equilibrium intermixing and phase transformation in severely deformed Al/Ni multilayers [J]. Scripta Materialia, 2007, 56(3): 181–184.
- [22] CHUNG C Y, ZHU M, MAN C H. Effect of mechanical alloying on the solid state reaction processing of Ni-36.5at.%Al alloy [J]. Intermetallics, 2002, 10(9): 865-871
- [23] SAUVAGE X, WETSCHER F, PAREIGE P. Mechanical alloying of Cu and Fe induced by severe plastic deformation of a Cu–Fe composite [J]. Acta Materialia, 2005, 53(7): 2127–2135.
- [24] SATO K, YOSHIIE T, SATOH Y, XU Q, KIRITANI M. Simulation of vacancy migration energy in Cu under high strain [J]. Materials Science and Engineering A, 2003, 350(1/2): 220–222.
- [25] LIU Teng, WANG Qu-dong, SUI Yu-dong, WANG Qi-gui, DING Wen-jiang. An investigation into aluminum—aluminum

- bimetal fabrication by squeeze casting [J]. Materials & Design, 2015, 68: 8-17.
- [26] LIU Ya-zhou, WANG Wen-yan, HUANG Ya-bo, XIE Jing-pei, GUO Lei-ming, ZHANG Miao-fei. Effect of annealing temperature on microstructure and bond strength of cast-rolling Cu–Al clad plates [J]. Materials Research Express, 2019, 6(8): 86556–86563.
- [27] LIU B X, YIN F X, DAI X L, HE J N, FANG W, CHEN C X, DONG Y C. The tensile behaviors and fracture characteristics of stainless steel clad plates with different interfacial status [J]. Materials Science and Engineering A, 2017, 679: 172–182.
- [28] CAO Miao, DENG Kun-kun, NIE Kai-bo, WANG Cui-ju, WANG Li-fei, LIANG Wei. Microstructure, mechanical properties and formability of Ti/Al/Ti laminated composites fabricated by hot-pressing [J]. Journal of Manufacturing Processes, 2020, 58: 322–334.
- [29] CHEN Ming-song, ZOU Zong-huai, LIN Y C, LI Hong-bin, WANG Guan-qiang, MA Yan-yong. Microstructural evolution and grain refinement mechanisms of a Ni-based superalloy during a two-stage annealing treatment [J]. Materials Characterization, 2019, 151: 445–456.
- [30] ZUO Yu-bo, FU Xing, CUI Jian-zhong, TANG Xiang-yu, MAO Lu, LI Lei, ZHU Qing-feng. Shear deformation and plate shape control of hot-rolled aluminium alloy thick plate prepared by asymmetric rolling process [J]. Transactions of Nonferrous Metals Society of China, 2014, 24(7): 2220–2225.
- [31] WANG Peng-ju, HUANG Hong-tao, LIU Jiang-jiang, LIU Qing, CHEN Ze-jun. Microstructure and mechanical properties of Ti<sub>6</sub>Al<sub>4</sub>V/AA6061/AZ31 laminated metal composites (LMCs) fabricated by hot roll bonding [J]. Journal of Alloys and Compounds, 2021, 861: 157943–157953.
- [32] GRYDIN O, STOLBCHENKO M, BAUER M, SCHAPER M. Asymmetric twin-roll casting of an Al-Mg-Si-alloy [J]. Materials Science Forum, 2018, 918: 48-53.

# Cu/Al 复合板双辊铸轧复合界面压力分布与结合特性

张俊鹏 1,2, 黄华贵 1,2, 孙静娜 1,2, 赵日东 1,2, 冯 淼 1,2

- 1. 燕山大学 国家冷轧板带装备及工艺工程技术研究中心,秦皇岛 066004;
  - 2. 燕山大学 机械工程学院,秦皇岛 066004

摘 要:双辊铸轧工艺制备双金属层复合板的力学性能和产品厚度规格与结合界面相互作用力学行为密切相关。以铸轧速度为变量,建立热流耦合模拟与界面压力分布计算模型。结果表明,随着铸轧速度的降低,界面温度降低,界面压力与出口铝侧厚度占比增大。铜带减薄主要发生在后滑移区。较高的界面压力和较长的固体/半固体接触时间使结合面充分浸润,为原子扩散提供有利条件。当铸轧速度为 2.4 m/min 时,扩散层宽度为 4.9 μm,剥离后铜侧表面被铝覆盖,铝侧发生韧性断裂,有效防止界面分层及裂纹扩展。同时,高界面压力及塑性应变下的剪切作用更显著,铝侧显微组织为细长柱状晶体。因此,结合界面实现冶金结合并细化铝侧晶粒可以使复合板获得较高的结合强度和拉伸性能。

关键词:铜/铝复合板;铸轧速度;复合界面;双辊铸轧